The membrane topology of the amino-terminal domain of the red cell calcium pump

ARTICLE *in* PROTEIN SCIENCE · AUGUST 1997

Impact Factor: 2.85 · DOI: 10.1002/pro.5560060811 · Source: PubMed

Protein Science (1997), 6:1708–1717. Cambridge University Press. Printed in the USA.

The membrane topology of the amino-terminal domain of the red cell calcium pump

PABLO R. CASTELLO, F. LUIS GONZÁLEZ FLECHA, ARIEL J. CARIDE,[1]
HORACIO N. FERNÁNDEZ,[2] JOSÉ M. DELFINO, AND JUAN P.F.C. ROSSI

Departamento de Química Biológica—IQUIFIB, Facultad de Farmacia y Bioquímica,
Universidad de Buenos Aires, Junín 956, 1113 Buenos Aires, Argentina

(RECEIVED February 14, 1997; ACCEPTED April 4, 1997)

Abstract

A systematic study of the membrane-associated regions in the plasma membrane Ca^{2+} pump of erythrocytes has been performed by hydrophobic photolabeling. Purified Ca^{2+} pump was labeled with 3-(trifluoromethyl)-3-(*m*-[^{125}I]iodophenyl)-diazirine ([^{125}I]TID), a generic photoactivatable hydrophobic probe. These results were compared with the enzyme labeled with a strictly membrane-bound probe, [^{3}H]bis-phosphatidylethanolamine (trifluoromethyl) phenyldiazirine. A significant light-dependent labeling of an M_r 135,000–140,000 peptide, corresponding to the full Ca^{2+} pump, was observed with both probes. After proteolysis of the pump labeled with each probe and isolation of fragments by SDS-PAGE, a common pattern of labeled peptides was observed. Similarly, labeling of the Ca^{2+} pump with [^{125}I]TID, either in isolated red blood cell membranes or after the enzyme was purified, yields a similar pattern of labeled peptides. Taken together, these results validate the use of either probe to study the lipid interface of the membrane-embedded region of this protein, and sustain the notion that the conformation of the pump is maintained throughout the procedures of solubilization, affinity purification, and reconstitution into proteoliposomes. In this work, we put special emphasis on a detailed analysis of the N-terminal domain of the Ca^{2+} pump. A labeled peptide of M_r 40,000 belonging to this region was purified and further digested with V8 protease. The specific incorporation of [^{125}I]TID to proteolytic fragments pertaining to the amino-terminal region indicates the existence of two transmembrane stretches in this domain. A theoretical analysis based on the amino acid sequence 1–322 predicts two segments with high probability of membrane insertion, in agreement with the experimental data. Each segment shows a periodicity pattern of hydrophobicity and variability compatible with α-helical structure. These results strongly suggest the existence of a transmembrane helical hairpin motif near the N-terminus of the Ca^{2+} pump.

Keywords: calcium pump; detection of the outside face of the helices; hydrophobic photolabeling; membrane proteins; secondary structure prediction for transmembrane segments; transmembrane topology

The erythrocyte Ca^{2+} pump is a monomeric integral membrane protein that actively transports Ca^{2+} from the cytoplasm to the external milieu. The main portion of the pump faces the cytoplasm. By contrast, it is believed that short external loops connect 8–10 putative transmembrane segments (Penniston & Enyedi, 1994; Stokes et al., 1994; Lutsenko & Kaplan, 1995; Møller et al., 1996).

Valuable experimental information on the topology of membrane proteins can be obtained with the help of photoactivatable reagents designed to react within the hydrophobic milieu of the lipid bilayer. Most successful reagents of this general type include the photolabeling group TPD, which generates a very reactive carbene species upon irradiation with UV light (Brunner, 1993).

We have employed [^{3}H]DIPETPD (Fig. 1A), a photochemical bipolar phospholipidic probe designed to label deeply into the lipid bilayer (Delfino et al., 1993), to explore the transmembrane organization of the Ca^{2+} pump (Castello et al., 1994). Therein we demonstrated the existence of three hydrophobic clusters along the sequence of the pump. These clusters include transmembrane regions of the pump, because labeling with [^{3}H]DIPETPD is restricted mainly to the middle plane of the lipid bilayer (Stegmann et al., 1991; Delfino et al., 1993).

Reprint requests to: Juan Pablo F.C. Rossi or José María Delfino, Departamento de Química Biológica—IQUIFIB, Facultad de Farmacia y Bioquímica, Universidad de Buenos Aires, Junín 956, 1113 Buenos Aires, Argentina; e-mail: rtjpaul@criba.edu.ar, rtdelfin@criba.edu.ar.

[1]Present address: Department of Biochemistry and Molecular Biology, Mayo Clinic Foundation, Rochester, Minnesota 55905.

[2]Deceased August 2, 1995.

Abbreviations: PMCA, plasma membrane calcium pump; [^{3}H]DIPETPD, [^{3}H]bis-phosphatidylethanolamine (trifluoromethyl) phenyldiazirine; [^{125}I]TID, 3-(trifluoromethyl)-3-(*m*-[^{125}I]iodophenyl)-diazirine; $C_{12}E_{10}$, polyoxyethylene 10 lauryl ether; DTT, 1,4-dithiothreitol; EGTA, ethylene glycol bis(β-aminoethyl ether)-*N*,*N*,*N*′,*N*′-tetraacetic acid; hPMCA4b, isoform 4b of the human plasma membrane calcium pump; M_1–M_{10}, proposed transmembrane segments in the hPMCA4b; MAb, monoclonal antibody; MOPS, 3-(*N*-morpholino)-propanesulfonic acid; PVDF, polyvinylidene difluoride; TPD, 3-trifluoromethyl-3-phenyl-diazirine.

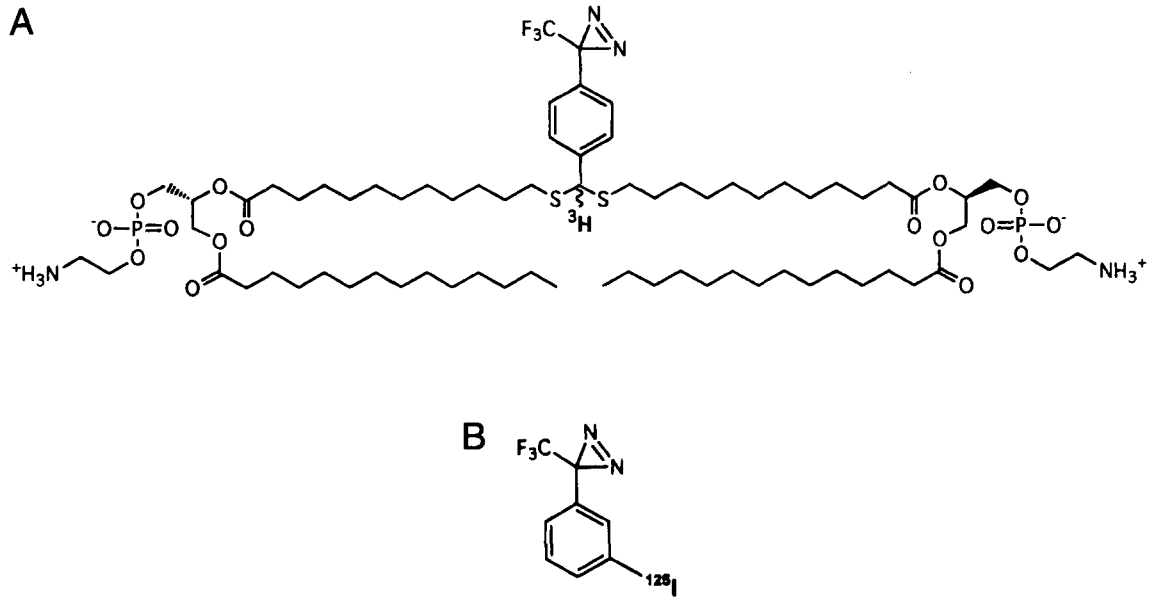

Fig. 1. Two hydrophobic photolabeling reagents [^{3}H]DIPETPD (**A**) and [^{125}I]TID (**B**).

The importance of the amino-terminal region of the Ca^{2+} pump cannot be underestimated. It has been shown that, after tryptic cleavage of the erythrocyte Ca^{2+} pump, a series of fragments ranging between M_r 90,000 and 76,000 demonstrated enzymatic activity (Zurini et al., 1984; Enyedi et al., 1987; Zvaritch et al., 1990). In particular, a fragment of M_r 76,000 lacking 358 amino acid residues from the N-terminus and 139 residues from the C-terminus appears to express calcium ATPase activity. This fragmented enzyme is devoid of calmodulin or acidic phospholipid modulation (Enyedi et al., 1987). According to this evidence, the N-terminal domain would not be critical for function. Conversely, Heim et al. (1992) expressed an M_r 105,000 fragment of this protein that does not include the N-terminal domain and demonstrated that it lacks enzymatic activity. More recently, Grimaldi et al. (1996) investigated the functional consequences of a deletion between residues 18 and 75 of the isoform hPMCA4b of the pump. This mutant was unable to transport Ca^{2+}, hydrolyze ATP, or form an intermediate phosphoenzyme. This apparent discrepancy may be explained as follows. The persistence of noncovalent associations between fragments may give rise to ensembles showing catalytic activity. On the other hand, alterations in folding and insertion in the mutant proteins could prevent proper functioning.

Given the current interest in this domain of the Ca^{2+} pump, in this paper we employ the hydrophobic photolabeling approach supported by theoretical amino acid sequence analysis to elucidate structural aspects of this protein.

Results

Labeling of Ca^{2+}-ATPase with [^{3}H]DIPETPD and [^{125}I]TID

The Ca^{2+} pump was reconstituted into liposomes and reacted with either [^{3}H]DIPETPD or [^{125}I]TID (Fig. 1A,B). After electrophoresis under denaturing conditions, both probes were shown to be bound covalently to the protein. A nonirradiated sample showed no significant incorporation of label (results not shown). In order to assess the extent of reaction of different regions of this protein with each hydrophobic probe, we then proceeded to determine the incorporation of label to proteolytic fragments of the pump. Figure 2A and B shows the extent of labeling with [^{3}H]DIPETPD and [^{125}I]TID, respectively, of fragments obtained after controlled proteolysis with V8 protease (4 h at 25 °C with 200 ng/mL of protease in the presence of 0.8% SDS). Five labeled bands were detected after staining the gel with colloidal Brilliant Blue G. Three of these bands correspond to peptides C, D, and E, which are nonoverlapping fragments spanning the whole sequence of the pump (see Fig. 6 and Table 1). Fragments D and C include the N and the C termini, respectively, and fragment E corresponds to a major central portion of this protein. Peptides A and B are transient precursors to these fragments.

Both [^{3}H]DIPETPD and [^{125}I]TID labeled these five peptides with a similar pattern. Given this result and the higher specific activity attainable with ^{125}I as compared with ^{3}H, we decided to pursue subsequent experiments with [^{125}I]TID. On the other hand, we tested this reagent in its ability to label the Ca^{2+} pump when the protein had been reconstituted into proteoliposomes with asolectin, or solubilized in micellar form, as resulted after the affinity purification step. After controlled proteolysis with V8 protease under the conditions described above, a similar distribution of radioactive label among peptides was obtained for both preparations (results not shown). Thus, all further experiments were performed on solubilized preparations of the Ca^{2+} pump.

To ultimately assess the validity of this experimental approach to probe conformational features of this membrane protein, we used [^{125}I]TID to label the Ca^{2+} pump on intact erythrocyte membranes, i.e., when this protein is surrounded by its natural phospholipidic milieu. Red blood cell membranes were labeled with [^{125}I]TID, and the Ca^{2+} pump was purified afterward by the usual procedure of affinity chromatography on a calmodulin–agarose column. The protein was then digested with V8 protease as described above, and, after separation by SDS-PAGE, the pattern of labeled peptides showed five radioactive bands, similar in position and size to those shown in Figure 2B (results not shown).

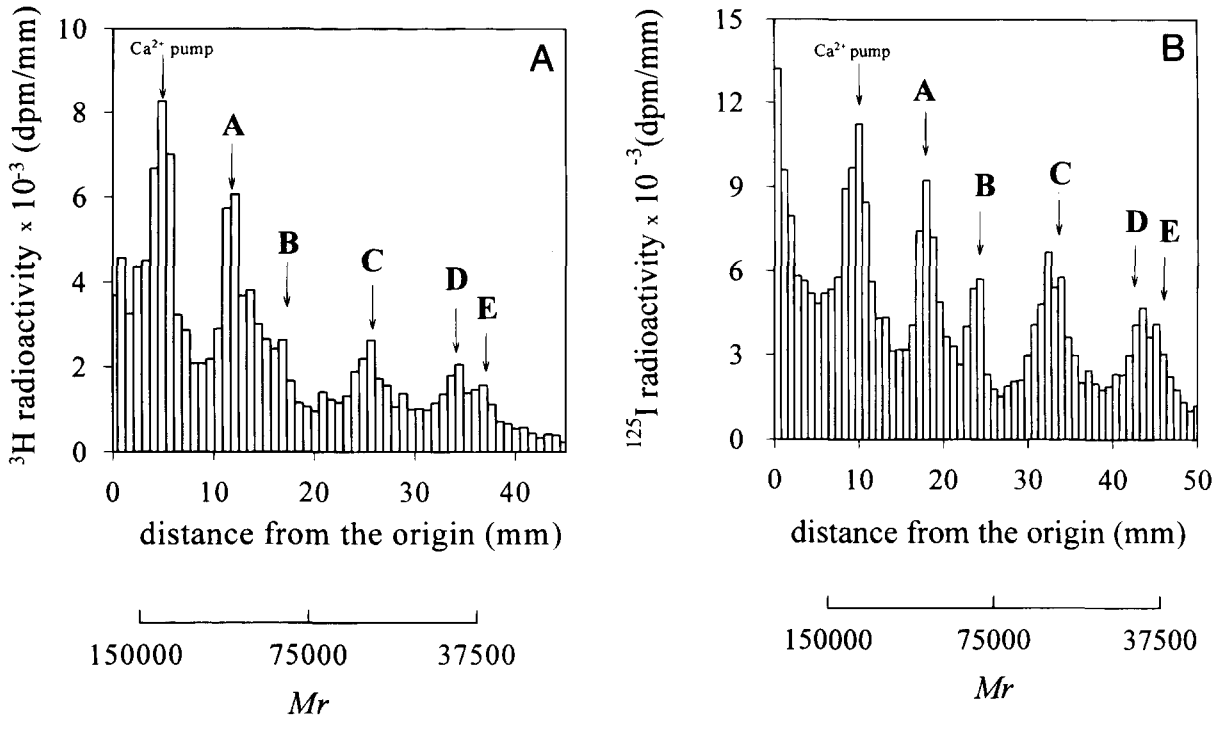

Fig. 2. Electrophoretic analysis of peptides obtained after V8 protease digestion of the plasma membrane calcium pump labeled with [^{3}H]DIPETPD (**A**) or [^{125}I]TID (**B**). Purified Ca^{2+}-ATPase (50–100 μg of protein/mL) was reconstituted into proteoliposomes loaded with 5 μCi of either photoactivatable probe. Each sample was then irradiated, dialyzed against 50 mM Tris-H_3PO_4 (pH 7.2 at 25 °C), and digested for 4 h with 200 ng/mL of V8 protease in the presence of 0.8% of SDS. The reaction was stopped by the addition of 3,4-dichloroisocoumarin up to a final concentration of 25 μM. The peptide mixture was separated by SDS-PAGE and the distribution of radioactivity in the gel was determined as described in Materials and methods. Arrows indicate the proteolytic fragments A–E.

Enrichment of a peptide that comprises the N-terminal region of the Ca^{2+} pump (peptide D)

The similar mobilities shown by peptides D and E impair their isolation in pure form by SDS-PAGE (Fig. 2B). In order to overcome the problem of cross contamination, novel conditions for digestion of the Ca^{2+}-ATPase were sought. In the absence of SDS, V8 protease yields peptides D and A as sole products (Fig. 3), i.e., under these conditions, V8 protease fails to split peptide A into E and C (see Fig. 6).

Table 1. *Peptide map of the Ca^{2+} pump digested with V8 protease*

Peptide		Reactivity with MAbs[a]	N-terminal sequencing	M_r ± SEM[b]	M_r[c]
Whole pump	(1–1205)	5F10-JA3-JA9	—	133,634 ± 2,222	133,945
A	(323–1205)	5F10-JA3	IQPLN	97,671 ± 1,400	98,688
B	(1–661)	JA9	N-blocked	79,688 ± 1,566	73,408
C	(662–1205)	5F10-JA3	LTCIA	57,727 ± 534	60,554
D	(1–322)	JA9	N-blocked	40,417 ± 445	35,274
E	(323–661)	NO	IQPLN	36,656 ± 453	38,151
F	(1–130)	JA9	N-blocked	15,006 ± 473	14,522
G	(131–322)	NO	LCGQV	22,358 ± 463	20,769
H	(1–236)	JA9	N-blocked	25,990 ± 524	26,173
I	(237–322)	NO	SSLTGE	10,353 ± 371	9,118

[a]JA9 reacts with the N-terminal region, comprising residues 17–75 in the hPMCA4b isoform of the pump. 5F10 reacts with the central portion of the protein, including residues 724–783; and JA3 reacts with the C-terminus of the pump, including residues 1135–1205 (Caride et al., 1996). NO means absence of reactivity against all three MAbs tested.

[b]Estimated by comparison with the mobilities of standard proteins simultaneously run on the same gel. Reported values are the average of seven independent experiments with the corresponding standard error of the mean.

[c]Estimated from the amino acid sequence, assuming contiguous peptides.

Subdigestion of the N-terminal fragment (peptide D) of [^{125}I]TID labeled Ca^{2+} pump

Proteolysis of peptide D allowed us to circumscribe the membrane-embedded regions located in this domain. After labeling of the Ca^{2+} pump with [^{125}I]TID and proteolysis with V8 protease under the conditions described in the legend to Figure 3, peptide D was isolated in pure form by SDS-PAGE. The peptide was eluted from the gel by diffusion with a recovery that was better than 90%. This sample was further digested for 15 h at 25 °C with 500 ng/mL of V8 protease in the presence of 0.8% SDS. An SDS-PAGE analysis of this digestion mixture revealed four major peptides: F, G, H, and I. Due to the similar mobilities of peptides G and H, and those of peptides F and I, each band was eluted and run a second time by SDS-PAGE. In the end, all four peptides were isolated in pure form, as judged by the appearance of a single stained band in each lane associated with the radioactivity peak (Fig. 4). Furthermore, Edman degradation of the peptide material eluted from each band yielded a single sequence.

Quantitative analysis of radioactivity incorporated into peptides belonging to the N terminus of [^{125}I]TID labeled Ca^{2+} pump

Figure 5 shows the incorporation of radioactivity from [^{125}I]TID to the whole Ca^{2+} pump, to peptide D, and to fragments obtained by subdigestion of peptide D, i.e., fragments F, G, H, and I, as a function of the amount of peptide. Increasing quantities of each labeled peptide were sampled on different lanes and run by SDS-PAGE. The amount of peptide and the incorporation of radioactivity were estimated as described in Materials and methods. All samples rendered straight lines that could be fitted to linear functions with nonsignificant intercepts. The slope of each curve provides a very accurate measure of the specific radioactivity of each peptide. The values calculated for each sample were the following: 183.9 ± 22 cpm/pmol, whole pump; 52.19 ± 1.6 cpm/pmol, fragment D; 22.4 ± 1.0 cpm/pmol, fragment F; 21.07 ± 1.25 cpm/pmol, fragment G; 36.09 ± 1.3 cpm/pmol, fragment H; and 4.35 ± 0.7 cpm/pmol, fragment I. A control sample of hen egg white lysozyme dissolved in storage buffer showed insignificant incorporation of label.

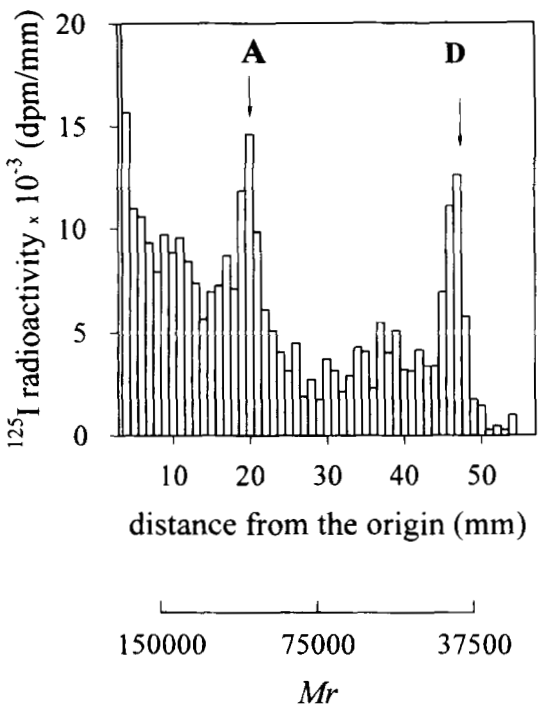

Fig. 3. Isolation of peptide D. Purified Ca^{2+} pump (50–100 μg of protein/mL) solubilized in $C_{12}E_{10}$/asolectin mixed micelles was labeled with [^{125}I]TID and dialyzed against 50 mM Tris-H_3PO_4 (pH 7.2 at 25 °C). The sample was digested with 200 ng/mL of V8 protease during 2 h in the absence of SDS. The peptide mixture was separated by SDS-PAGE and the distribution of radioactivity in the gel was determined as described in Materials and methods. Arrows indicate the positions where the proteolytic fragments A and D appear in the gel.

Characterization of the fragments of the Ca^{2+} pump obtained after proteolysis with V8 protease

Peptides A–I, obtained after proteolysis with V8 protease under the different conditions described above and isolated by SDS-PAGE, were characterized by both (1) reaction with MAbs and (2) microsequencing techniques (Table 1). Positive identification of each fragment was possible by the availability of three MAbs, JA9, 5F10, and JA3, directed against different epitopes of the pump. In addition, successful chemical microsequencing of most peptides was achieved after blotting into PVDF membranes. The only exceptions were those peptides comprising the N-terminus of the protein, which is assumed to be acetylated (Carafoli, 1991). A consistent peptide pattern accounting for the full amino acid sequence of the Ca^{2+} pump emerges by relating the N-terminal sequence information with the molecular mass of each fragment, as estimated by SDS-PAGE (Fig. 6).

Theoretical analysis of the amino acid sequences corresponding to the putative transmembrane segments belonging to HC1

Hydropathy analysis of the N-terminal domain of the calcium pump, using the hydrophobicity scales of Kyte and Doolittle (1982), and Goldman, Engelman, and Steitz (Engelman et al., 1986), predicted two distinct zones with a high likelihood for membrane insertion, namely, segments 100–122 and 150–168 according to the former, and 105–119 and 153–166 according to the latter. In particular, stabilizing ion pairs at $i + 4$ or $i + 5$ were conspicuously absent in these regions.

Independently, two other algorithms rendered similar results, i.e., TMAP (Persson & Argos, 1994) predicted segments 96–124 and 147–169, and PHD (Rost et al., 1995) did so for segments 103–120 and 151–168. The amino acid sequence of isoform hPMCA4b of the calcium pump, well aligned by homology with a representative set of type II P-ATPases, was the input to the latter algorithm. In order to construct this set, we selected between one and three members of each branch in the phylogenetic tree proposed by Møller et al. (1996). We always included one example of each major isoform present in Swiss-Prot, and set the highest priority on the human sequences (if any appeared in this data bank). In their absence, the highest homologous sequences to the hPMCA4b isoform (atcr_human) were chosen. In the end, the selected sequences, extracted from Swiss-Prot, were: atcr_human, atcp_rat, atcp_human, atcq_human, atc3_yeast, atcb_chick, atcd_human, atc1_yeast, atcl_synp7, ata1_syny3, atce_human, atn3_human, atcf_rat, atn2_human, atn1_human, atha_human, atma_salty, pma1_neucr, pma1_arath, pma3_arath, and pma2_arath.

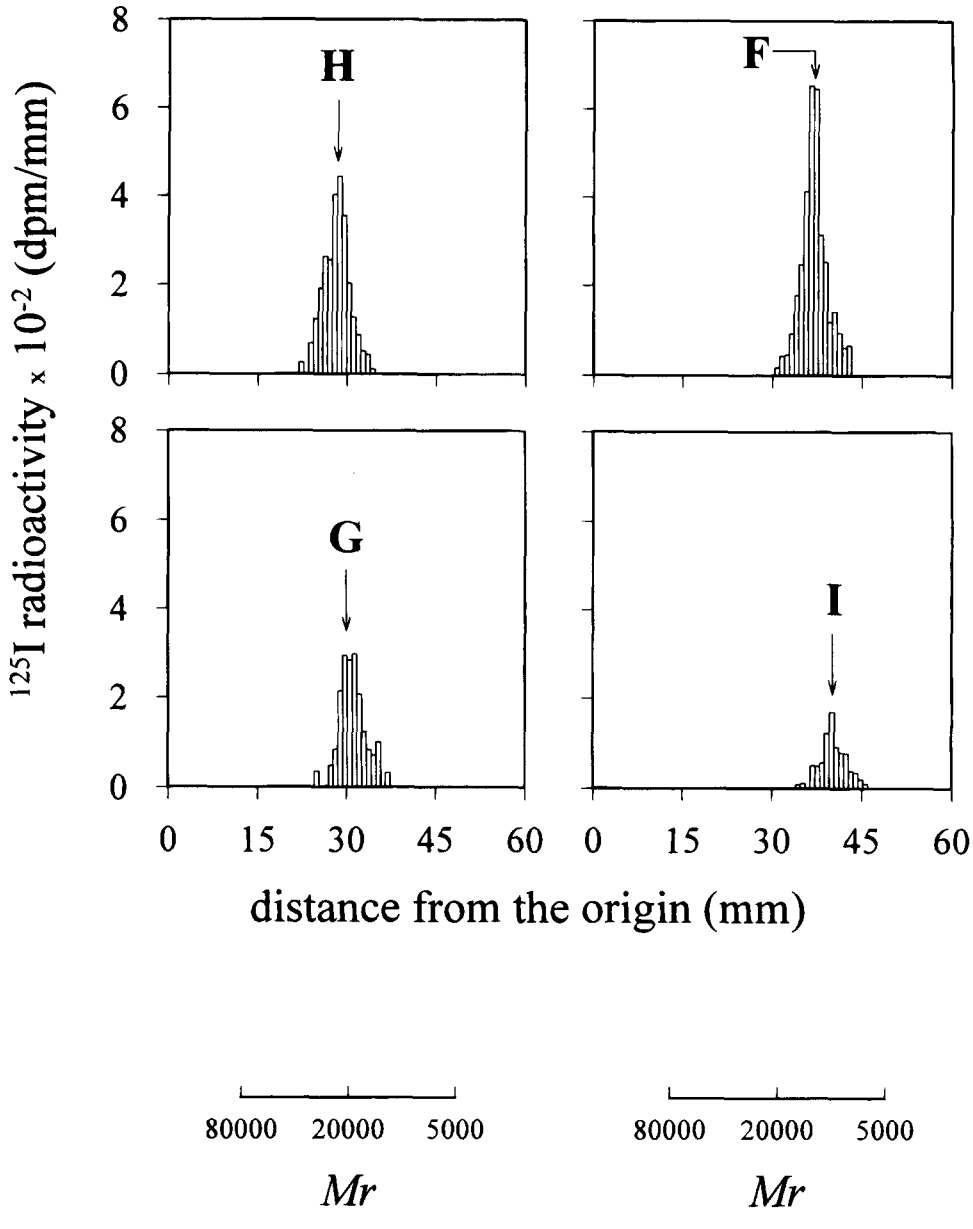

Fig. 4. Subdigestion of fragment D. Peptide D (50–100 μg/mL) was obtained as described in the legend to Figure 3. After SDS-PAGE, the peptide bands become evident by reverse staining. Peptide D was then eluted by diffusion. This sample was further digested for 15 h with 500 ng/mL of V8 protease in 50 mM Tris-H_3PO_4 (pH 7.2 at 25 °C) in the presence of 0.8% SDS. The resulting peptides were separated by SDS-PAGE, eluted, and re-purified by the same technique. Peptides H (1.42 μg), G (1.31 μg), F (1.47 μg), and I (1.25 μg) were sampled in separate lanes. The distribution of radioactivity in the gel was determined as described in Materials and methods. Arrows indicate positions where the proteolytic fragments F, G, H, and I appear in the gel.

Secondary structure predictions according to Chou and Fasman (1978), Garnier, Osguthorpe, and Robson (Garnier et al., 1978), and PHD (Rost & Sander, 1993, 1994) suggested that M1 has a definite alpha-helical character. On the other hand, assignment of secondary structure for M2 is less clear, because the three algorithms assayed predicted comparable proportions of alpha and beta structures. Nevertheless, PHD interpreted that a major central portion of M2 should be alpha helical. Because secondary structure prediction schemes using a database of soluble proteins (Chou & Fasman, 1978; Garnier et al., 1978) appear to be less appropriate for the prediction of membrane protein folding (Wallace et al., 1986), we decided to evaluate the propensity for helix formation on the basis of hydrophobicity and variability functions (μ_H and μ_V, respectively, Equation 1):

$$\mu_{H,V}(\delta) = \frac{1}{N}\left\{\left[\sum_{j=1}^{N} F_j \cos(j\delta)\right]^2 + \left[\sum_{j=1}^{N} F_j \sin(j\delta)\right]^2\right\}^{1/2}. \quad (1)$$

N is the number of amino acids of the segment under analysis and δ is the angle between successive Cα viewed down the central axis of the assumed structure. δ ranges between 0 and 180°.

For μ_H, the hydrophobicity (H) values were taken from the consensus scale of Eisenberg et al. (1984a) and $F_j = H_j - \langle H \rangle$ (solid lines in Fig. 7A,B). Independently, by using the set of well-

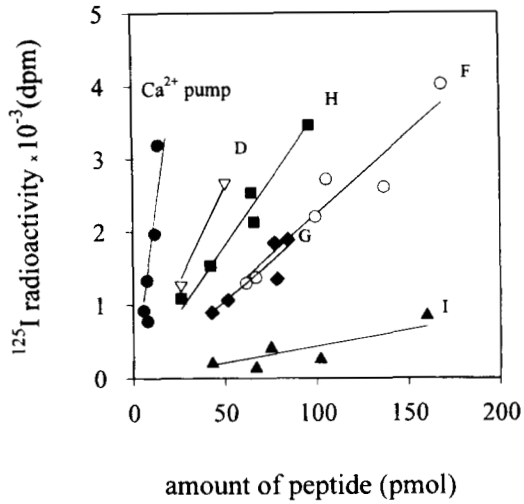

Fig. 5. Specific radioactivity of peptides derived from fragment D. Total amount of peptide in each band and total radioactivity incorporated into each peptide were estimated as described in Materials and methods. Peptides F (○), G (♦), H (■), and I (▲) were plotted. Data corresponding to each peptide were fitted by linear regression (solid line). For the purpose of comparison, the specific radioactivity of the whole calcium pump (●) and of peptide D (▽) were also included.

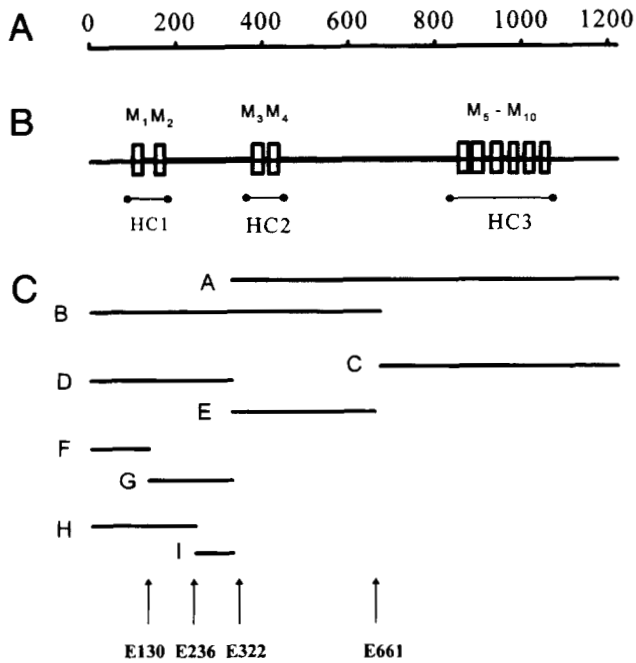

Fig. 6. Proteolytic map of Ca^{2+}-ATPase digested with V8 protease. Upper rule (**A**) shows the positions along the amino acid sequence. Boxed regions along the line (**B**) indicate the consensus location of putative transmembrane segments M_1–M_{10}, defining the three hydrophobic clusters, HC1, HC2, and HC3 (underlines). Peptides A–I, obtained after V8 protease digestion of the calcium pump, are indicated with segments (**C**). Sites of V8 protease cleavage are indicated below with arrows.

aligned sequences of type II P-ATPases described above, we established a measure of allowed variability (V) from the number of point mutations at all amino acid positions of the putative transmembrane stretches. The variability function (μ_V) was then calculated in the same fashion as described before for the hydrophobic function, where $F_j = V_j - \langle V \rangle$ (dashed lines in Fig. 7A,B). These functions allowed us to explore the periodicity in both properties on all possible δ angles. The choice of the most likely secondary structure for one segment is made on the basis of the value of the δ angle that maximizes this function. With these values of δ, the hydrophobic and variability moments were then calculated. The cartesian components of each vector are given by the sum terms in Equation 1.

For M1, both functions maximize at angles of 102° (μ_H) and 105° (μ_V), very close to the angle characteristic of a canonical alpha helix (100°). The inset to Figure 7A shows both the hydrophobic and the variability moments on a helical wheel representation of M1. μ_H has a modulus (given by Equation 1) of 0.29 and points to Val 104 in the axial projection, whereas μ_V has a modulus of 0.69 and points to a position between Ile 107 and Val 118. The directions of both vectors do not differ much, i.e., the angle between them is 52°. With reasonably high likelihood, these data support the notion that M1 could adopt an amphipathic alpha helical structure, where the most hydrophobic face shows the highest variability.

For M2, the periodicity of hydrophobic and variable positions along this stretch is roughly the same (Fig. 7B), i.e., the hydrophobic and variation functions maximize at 95° and 98°, respectively. The moduli of the hydrophobic and variation moments are 0.17 and 0.70, respectively, and both point approximately in a direction between Ala 153 and Leu 164 in the helical wheel projection (the angle between them is 8.5°). Here again, these parameters suggest that a similar description to that given above for M1 can be drawn for M2.

Discussion

Hydrophobic photolabeling of the Ca^{2+} pump reveals topographic features of transmembrane domains

In a previous work (Castello et al., 1994), we employed [^{3}H]DIPETPD, a photochemical bipolar phospholipidic probe designed to label deeply into the lipid bilayer (Delfino et al., 1993), for exploring the transmembrane organization of the Ca^{2+} pump. In that study, we established the existence and location of three hydrophobic clusters (HC) along the sequence of the pump: HC1, HC2, and HC3 (Fig. 6). Because labeling with [^{3}H]DIPETPD is mainly restricted to the middle plane of the lipid bilayer (Stegmann et al., 1991; Delfino et al., 1993), the hydrophobic clusters referred to above necessarily include transmembrane regions of the pump.

After having identified unambiguously membrane-spanning stretches with [^{3}H]DIPETPD, we took advantage of the higher specific activity provided by the radioactive iodine tag present in [^{125}I]TID, a generic hydrophobic probe, to undertake further labeling experiments. The high extent of incorporation of radioactive label into peptides, achievable with [^{125}I]TID, allowed us to carry out the subdigestion of large fragments, in an attempt to increase the resolution at the locale of labeling. In this regard, it has been proven for other integral membrane proteins that the peptide labeling patterns do not differ much between phospholipid-based reagents bearing TPD [such as [^{3}H]PTPC/11 (Harter et al., 1989)] and [^{125}I]TID, implying that the role of the chemistry of the reagent prevails over the position where the probe function is attached (Meister et al., 1985; Harter et al., 1989). Labeling experiments conducted in our laboratory showed that this is also the case for the

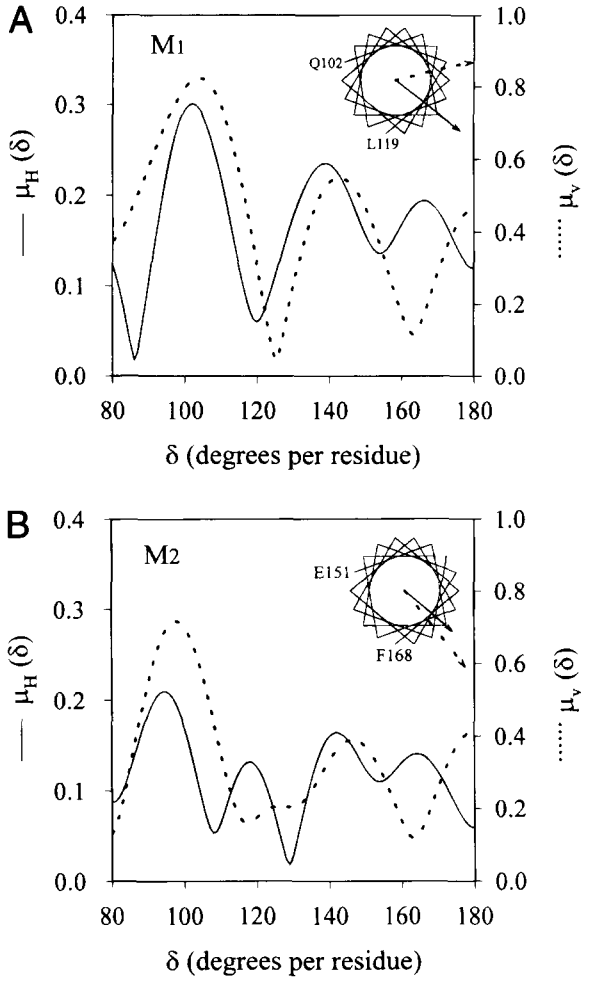

Fig. 7. Hydrophobic and variability functions for the proposed transmembrane segments belonging to the N-terminal region of the plasma membrane Ca^{2+} pump. The hydrophobic function μ_H and the variability function μ_V were calculated according to Equation 1 for the putative transmembrane segments M1 (**A**) and M2 (**B**). The hydrophobic (solid arrow) and variability (dashed arrow) moments for the helices are represented in the insets.

Ca^{2+} pump reconstituted into lipid vesicles. As shown in Figure 2A and B, the two hydrophobic probes assayed here, namely [^{3}H]DIPETPD and [^{125}I]TID, yield similar profiles for the labeled peptides. After controlled proteolysis of the Ca^{2+} pump with V8 protease, patterns of labeled peptides were compared in experiments where we modified the lipidic milieu of the pump. Results are similar when the enzyme is labeled with [^{125}I]TID, either in its natural environment ("in situ" labeling on red blood cell ghosts, results not shown) or in lipid-detergent micelles (Fig. 2B). Hence, it can be concluded that the experimental procedures of solubilization, purification, and reconstitution of the Ca^{2+} pump do not introduce major changes in the transmembrane organization of this protein. In addition, the preservation of transport activity in reconstituted liposomes (Castello et al., 1994) and the maintenance of the kinetic properties and regulatory characteristics in the purified enzyme (Kosk-Kosicka, 1990) support this view. These experiments validate hydrophobic photolabeling as a method to address the conformational analysis of the Ca^{2+} pump.

The first hydrophobic cluster (HC1) includes two distinct transmembrane segments, M1 and M2

In this paper, we focus on the analysis of the first hydrophobic cluster HC1 (see Fig. 6), located close to the N-terminal end of the protein. In the absence of SDS, V8 protease yields peptides D and A as sole products (Fig. 3). The high extent of labeling of peptide D, comprising the membrane-embedded regions located at the N-terminal domain, allowed us to conduct further fragmentation with the purpose of isolating peptides including single transmembrane stretches. Indeed, peptide D was subdigested with V8 protease under more severe conditions to yield peptides F and G, which comprise putative transmembrane segments M1 and M2, respectively.

Two pieces of data exist in the literature that complement our results: (1) Caride et al. (1996) determined the precise location of the epitopes for antibodies JA9, 5F10, and JA3, all directed against intracellular sites; and (2) Feschenko et al. (1992) found an extracellular loop that acts as an epitope to antibody 1E4 (Glu 130–Glu 142). We found the first cleavage site of V8 protease at the beginning of this segment (Glu 130). The distance between the epitope recognized by JA9 (which ends at Lys 75) and the cleavage site is long enough to accommodate only one transmembrane segment in fragment F. This would correspond to the putative transmembrane segment M1. Similarly, the distance between the first (Glu 130) and second (Glu 236) cleavage sites with V8 protease would allow the existence of one or three transmembrane segments in fragment G. However, the extent of labeling with [^{125}I]TID of peptide G is comparable to that of peptide F, supporting the idea that only one transmembrane segment indeed exists. This would correspond to the putative transmembrane segment M2.

The fact that peptides F and G were labeled with a similar specific activity indicates that HC1 consists of two distinct membrane-embedded domains, each comprising a single transmembrane segment with comparable exposure to the lipid phase. For M1 and M2, this conclusion becomes valid after considering the absence of S-containing amino acids (Met or Cys) and the presence of one Trp residue at the edge of each segment. Therefore, no bias due to the specific chemical reactivity of the carbene versus nucleophilic amino acids is expected. In this fashion, an attempt could be made at interpreting the extent of [^{125}I]TID labeling as proportional to the area of the lipid–protein interface.

Further conclusions can be drawn from the quantitative analysis of the slopes of the curves (specific radioactivities of labeled peptides) shown in Figure 5. Radioactivity incorporated into peptide H is roughly equivalent to that expected for the sum of an equimolar mixture of peptides F and G; and, in turn, this value is also similar to the experimentally determined radioactivity incorporated into peptide D. These results are consistent with the fact that both peptides D and H include the same transmembrane segments (M1 and M2).

On the other hand, the slope corresponding to the whole pump is consistent with the presence of between 8 and 10 transmembrane segments, in agreement with the current models for the calcium pump (Penniston & Enyedi, 1994; Stokes et al., 1994; Møller et al., 1996). However, in this particular case, one should bear in mind that differential exposure to the lipid phase and/or the presence of unusually reactive side chains could bias the interpretation of this piece of data. Further analysis currently underway in our laboratory focuses on the individual contribution to the overall labeling of each transmembrane segment belonging to the other two hydrophobic clusters, i.e., HC2 and HC3.

Finally, the low specific activity shown by peptide I is not compatible with the existence of a transmembrane segment in this region. Again, this fact fits well with our own predictions, which do not support the existence of a transmembrane domain in this region, and with the assumed intracellular location for this segment in the standard models for the pump (Penniston & Enyedi, 1994; Stokes et al., 1994; Møller et al., 1996). It is possible (although unlikely) that the residual radioactivity present in this fragment could correspond to labeling of a hypothetical site for hydrophobic ligands. This would not be exceptional, because positive labeling with [^{125}I]TID has been demonstrated for the globular protein calmodulin (Krebs et al., 1984), and for specific sites within the channel of the nicotinic receptor (White et al., 1991).

M1 and M2 form a helical hairpin motif with a substantial area exposed to the lipid phase

According to the two-stage model for membrane protein folding, independently stable trans-bilayer helices interact to form the tertiary fold of the polypeptide chain (Popot & Engelman, 1990). In connection with this assumption, reasonable confidence should be given to predictions based on a partial amino acid sequence of a membrane-spanning domain of an integral membrane protein, because local interactions should dominate and determine the fold of the region. Upon this corollary, we undertook the task of predicting secondary structure and supersecondary arrangement for the first hydrophobic cluster of the erythrocyte calcium pump.

After the analysis of periodicity in hydrophobicity of segments of well-known protein structures, Eisenberg et al. (1984b) found that each region takes up the secondary structure that yields the largest possible value for the hydrophobic moment. A similar observation was reported by Komiya et al. (1988) for the variation moment, which points toward the side of a structure that experiences the highest number of replacements of amino acid residues over the course of evolutionary time. The hydrophobic and variability function profiles calculated for M1 and M2 (Fig. 7A,B) are comparable to those found for model peptides that should ideally fold as alpha helices, and for alpha helices present in known proteins (Eisenberg et al., 1984b; Komiya et al., 1988; Donnelly et al., 1993). In all cases, a prominent peak is observed at $\delta \sim 100°$, the characteristic angle of alpha-helical secondary structure.

Once the secondary structure had been assigned, the hydrophobic and the variability moments could be calculated. The angular deviation between these vectors is small, both for M1 and M2 (insets to Fig. 7A,B), in agreement with the notion that the outer, lipid-exposed surface of the membrane-embedded domain accommodates amino acid changes more readily than the inner, closed-packed surfaces. This is a characteristic feature of amphipathic transmembrane helices where the highly variable and the most hydrophobic faces overlap and are likely to be exposed to membrane lipids. Conversely, for surface helices in globular proteins, the directions of the two moments are opposed (Rees et al., 1989; Lüthy & Eisenberg, 1992). In addition, the mean hydrophobicity value and the magnitude of the hydrophobic moment calculated for M1 ($\langle H \rangle = 0.7$; $|\mu_H| = 0.26$) and M2 ($\langle H \rangle = 0.8$; $|\mu_H| = 0.17$) map to the region indicative of multimeric membrane-embedded alpha-helical bundles, as proposed by Eisenberg (1984), this being a common feature of many transport proteins.

After the considerations noted above, a clear picture emerges from the theoretical analysis of the N-terminal domain of the Ca^{2+} pump. At this level of study and in the absence of more detailed structural information, M1 and M2 can be visualized as cylinders with two differentiated faces: one with high hydrophobicity and variability, substantially exposed to membrane lipids, and the other possibly involved in specific protein–protein contacts important for the structural stability of the helix bundle.

The experimental counterpart to this analysis is the fact that both M1 and M2 are labeled significantly and to a similar extent with reagents that probe the lipid–protein interface, such as [^{3}H] DIPETPD and [^{125}I]TID. On the other hand, the hydrophilic stretch connecting M1 and M2 includes a site susceptible to cleavage with V8 protease. This fact is consistent with the presence of an outer loop exposed to the aqueous solvent. This region is accessible to proteases under exhaustive conditions, and includes the epitope to antibody 1E4, as demonstrated by Feschenko et al. (1992).

In a number of instances, the "positive inside rule," established originally for bacterial inner membrane proteins, can also be extended to eukaryotic membrane proteins (Sipos & von Heijne, 1993; von Heijne, 1994). Using this criterion, topology predictions of the transmembrane segments performed with PHD (Rost et al., 1996) reaffirm the proposed orientation of M1 and M2, i.e., two helices with the interhelical segment located outside the cell. This connecting stretch of 30 amino acids bears one positively charged (Arg 123) and seven negatively charged groups, in agreement with the extremely low frequency of positively charged amino acid residues observed in outer loops. By contrast, the intracellular flanking sequences are rich in positively charged amino acids.

A consistent picture emerges for the topography of the N-terminal domain of the Ca^{2+}-pump. Putting together these pieces of data, we propose that a helical hairpin motif exists at the N-terminus of this protein. This hairpin may adopt a peripheral location in the transmembrane bundle, therefore exhibiting a substantial boundary region with surrounding membrane phospholipids. Interestingly, Stokes et al. (1994) hypothesized a number of packing arrangements for the 10 helices belonging to the transmembrane domain of P-type ion pumps by model building on the basis of cryo-electron microscopy data at 14 Å resolution of the sarcoplasmic reticulum calcium pump (Toyoshima et al., 1993). All of these alternative models position M1 and M2 side by side at the interface with membrane lipids.

A natural extension of this work will include a similar analysis as that described in this paper for transmembrane segments belonging to HC2 and HC3. In addition, the availability of specific cleavage sites in the water-accessible regions of this protein could open the way to studies of fragment assembly in the membrane environment. Results of hydrophobic photolabeling experiments of the isolated fragments compared with noncovalent complexes could provide information on the structural features of the interaction between the different intramembranous domains of this protein.

Materials and methods

Materials

All the chemicals used in this work were of analytical grade and purchased mostly from Sigma Chemical Co. (USA). [^{3}H] DIPETPD was prepared as described previously (Delfino et al., 1993). [^{125}I]TID (2.8 mCi/mL in methanol:water, 3:1, v/v) was bought from Amersham International plc (UK). Recently drawn human blood for the isolation of Ca^{2+}-ATPase was obtained from the Hematology Section of the Hospital de Clínicas General San

Martín (Argentina). SDS-PAGE standards (broad range) were purchased from Bio Rad Laboratories (USA).

Purification of the Ca^{2+}-ATPase from human erythrocytes

Calmodulin-depleted erythrocyte membranes were prepared using a hypotonic solution (Gietzen et al., 1981). Ca^{2+}-ATPase was isolated in pure form by the calmodulin affinity chromatography procedure (Roufogalis & Villalobo, 1989) in the presence of asolectin and $C_{12}E_{10}$ and found to be homogeneous by SDS-PAGE (single band at M_r 134,000). The enzyme (50–100 μg/mL) was kept in storage buffer: 0.1% asolectin, 0.05% $C_{12}E_{10}$, 130 mM KCl, 20 mM MOPS-K, pH 7.2 at 4 °C, 1 mM $MgCl_2$, 2 mM EDTA, 2 mM $CaCl_2$, 2 mM DTT. ATPase activity was assayed according to González Flecha et al. (1993). Fractions showing the highest specific ATPase activity were pooled together. Protein concentration was determined according to Peterson (1977).

Photolabeling procedures

[^{3}H]DIPETPD was co-incorporated with the Ca^{2+} pump into liposomes, as described previously (Castello et al., 1994). Following an established procedure (Rao et al., 1991), [^{125}I]TID was incorporated directly to either (1) erythrocyte membranes, (2) purified calcium pump in micellar form, or (3) proteoliposomes of the calcium pump and phospholipids. Photoactivation was performed by irradiation at 366 nm for 20 min with a Desaga UVIS setup (C. Desaga, Germany).

Proteolysis of the Ca^{2+} pump

The enzyme was fragmented into peptides by digestion with V8 protease in 50 mM Tris-H_3PO_4 at pH 7.2 and 25 °C. Specific conditions for proteolysis are described in the legends to Figures 2, 3, and 4, and in Results.

PAGE

Electrophoresis was performed according to the Tris/tricine SDS/PAGE method (Schägger & von Jagow, 1987). Peptide bands were stained with colloidal Brilliant Blue G (Neuhoff et al., 1988), and accurate quantification of peptide amount was performed by densitometric analysis (González Flecha, 1996). The gel was dried and cut into slices 0.8-mm wide. For samples containing ^{3}H, after soaking each slice in hydrogen peroxide and incubation overnight at 50 °C (Tishler & Epstein, 1968), the radioactivity was determined by liquid scintillation counting. For samples containing ^{125}I, the radioactivity was measured by solid scintillation counting on the dried slices. A background correction was performed by subtracting the average radioactivity for gel slices containing no peptidic material. For purified peptides, no significant background radioactivity was measured. The radioactivity associated with each peptide was measured by estimating the area under a gaussian function fitted to the radioactivity distribution.

Isolation of selected peptide fragments

After electrophoresis, the gels were dyed according to the reverse staining method (Ferreras et al., 1993), except that we avoided the toning step to prevent protein aggregation. Polypeptide bands were cut and eluted by diffusion using a modification of a conventional method (Dzandu et al., 1988). The smashed gel was washed three times with 2 mL of 15 mM Tris-H_3PO_4, pH 7.4 at 25 °C, 0.25 mM EDTA, and 0.1% SDS per mL of gel.

Peptide identification

After SDS-PAGE, peptides were transferred to membranes by a semi-dry method (Laurière, 1993). Nitrocellulose membranes (Sigma Chemical Co., USA, pore size 0.2 μm) were used for immunostaining with a set of monoclonal antibodies directed toward different epitopes of the Ca^{2+} pump (Caride et al., 1996). Definitive identification of each peptide was performed by N-terminal sequencing after blotting the gel into PVDF membranes (Immobilon-P, Millipore Corporation, USA) on an Applied Biosystems 477 sequencer at the local protein facility (LANAIS-PRO, UBA-CONICET).

Theoretical analysis of the amino acid sequence

All calculations were performed on the reported amino acid sequence of the hPMCA4b isoform of the Ca^{2+} pump (Strehler et al., 1990), or on a representative set of 20 sequences of type II P-ATPases extracted from Swiss-Prot (see Results). Multiple sequence alignment was performed using a position-weighted dynamic programming method [MaxHom, EMBL, Heidelberg (Sander & Schneider, 1991)]. Prediction of transmembrane segments was conducted by hydropathy analysis, propensity values based on sequence homology, and a neural network algorithm. Two methods were used for the hydropathy analysis: (1) Kyte and Doolittle (1982), with an 11-residue window; and (2) a free energy difference calculation according to Goldman, Engelman, and Steitz (Engelman et al., 1986), which takes into account the burial inside the membrane of contact surface area and the formation of intrahelical ion pairs. Propensity values based on multiply aligned sequences were calculated with TMAP [EMBL, Heidelberg (Persson & Argos, 1994)]. The neural network algorithm employed was PHD [EMBL, Heidelberg (Rost et al., 1995)]. Secondary structure predictions were performed according to Chou and Fasman (1978) or GOR (Garnier et al., 1978) algorithms, as implemented in Protean (DNASTAR, Inc., Madison, Wisconsin, USA). Independently, a prediction method based on sequence profile input to neural networks [PHD, EMBL, Heidelberg (Rost & Sander, 1993, 1994)] was also applied. Periodicity in the hydrophobicity of the putative transmembrane segments was assessed through the hydrophobicity function, as described by Eisenberg et al. (1984b). Periodicity of conserved/variable residues in multiply aligned sequences was determined by evaluating the variability function, as described by Komiya et al. (1988), adopting some of the modifications proposed by Donnelly et al. (1993).

Acknowledgments

This work was supported by Consejo Nacional de Investigaciones Científicas y Técnicas (Res 2343/95-020), UBACYT (FA 046 and 003), and Fundación Antorchas (A 13359/1-106). We are indebted to Susana Linskens and Evangelina Dacci for technical support in peptide sequencing.

References

Brunner J. 1993. New photolabeling and crosslinking methods. *Annu Rev Biochem 62*:483–514.

Carafoli E. 1991. Calcium pump of the plasma membrane. *Physiol Reviews 71*:129–153.

Caride AJ, Filoteo AG, Enyedi A, Verma AK, Penniston JT. 1996. Detection of isoform 4 of the plasma membrane calcium pump in human tissues by using isoform-specific monoclonal antibodies. *Biochem J 316*:353–359.

Castello PR, Caride AJ, González Flecha FL, Fernández HN, Rossi JPFC, Delfino JM. 1994. Identification of transmembrane domains of the red cell calcium pump with a new photoactivatable phospholipidic probe. *Biochem Biophys Res Commun 201*:194–200.

Chou PY, Fasman GD. 1978. Prediction of the secondary structure of proteins from their amino acid sequence. *Adv Enzymol Relat Areas Mol Biol 47*:45–148.

Delfino JM, Schreiber SL, Richards FM. 1993. Design, synthesis, and properties of a photoactivatable membrane-spanning phospholipidic probe. *J Am Chem Soc 115*:3458–3474.

Donnelly D, Overington JP, Ruffle SV, Nugent JHA, Blundell TL. 1993. Modeling alpha-helical transmembrane domains: The calculation and use of substitution tables for lipid-facing residues. *Protein Sci 2*:55–70.

Dzandu JK, Johnson JF, Wise GE. 1988. Sodium dodecyl sulfate-gel electrophoresis: Staining of polypeptides using heavy metal salts. *Anal Biochem 174*:157–167.

Eisenberg D. 1984. Three-dimensional structure of membrane and surface proteins. *Annu Rev Biochem 53*:595–623.

Eisenberg D, Schwarz E, Komaromy M, Wall R. 1984a. Analysis of membrane and surface protein sequences with the hydrophobic moment plot. *J Mol Biol 179*:125–142.

Eisenberg D, Weiss RM, Terwilliger TC. 1984b. The hydrophobic moment detects periodicity in protein hydrophobicity. *Proc Natl Acad Sci USA 81*:140–144.

Engelman DM, Steitz TA, Goldman A. 1986. Identifying nonpolar transbilayer helices in amino acid sequences of membrane proteins. *Annu Rev Biophys Biophys Chem 15*:321–353.

Enyedi A, Flura M, Sarkadi B, Gardos G, Carafoli E. 1987. The maximal velocity and the calcium affinity of the red cell calcium pump may be regulated independently. *J Biol Chem 262*:6425–6430.

Ferreras M, Gavilanes JG, García-Segura JM. 1993. A permanent Zn^{2+} reverse staining method for the detection and quantification of proteins in polyacrylamide gels. *Anal Biochem 213*:206–212.

Feschenko MS, Zvaritch EI, Hofmann F, Shakhparonov MI, Modyanov NN, Vorherr T, Carafoli E. 1992. A monoclonal antibody recognizes an epitope in the first extracellular loop of the plasma membrane Ca^{2+} pump. *J Biol Chem 267*:4097–4101.

Garnier J, Osguthorpe DJ, Robson B. 1978. Analysis of the accuracy and implications of simple methods for predicting the secondary structure of globular proteins. *J Mol Biol 120*:97–120.

Gietzen K, Wüthrich A, Bader H. 1981. R 24571: A new powerful inhibitor of red blood cell Ca^{++}-transport ATPase and of calmodulin-regulated functions. *Biochem Biophys Res Commun 101*:418–425.

González Flecha FL. 1996. Estudio de las alteraciones producidas en la Ca^{2+}-ATPasa de eritrocitos humanos por glucosilacion no enzimática (Alterations in the human erythrocyte calcium pump produced by non enzymic glycation) [thesis]. Buenos Aires: Universidad de Buenos Aires.

González Flecha FL, Castello PR, Caride AJ, Gagliardino JJ, Rossi JPFC. 1993. The erythrocyte calcium pump is inhibited by non-enzymic glycation: Studies in situ and with the purified enzyme. *Biochem J 293*:369–375.

Grimaldi ME, Adamo HP, Rega AF, Penniston JT. 1996. Deletion of amino acid residues 18–75 inactivates the plasma membrane Ca^{2+} pump. *J Biol Chem 271*:26995–26997.

Harter C, James P, Bachi T, Semenza G, Brunner J. 1989. Hydrophobic binding of the ectodomain of influenza hemagglutinin to membranes occurs through the "fusion peptide." *J Biol Chem 264*:6459–6464.

Heim R, Iwata T, Zvaritch E, Adamo HP, Rutishauser B. Strehler EE, Guerini D, Carafoli E. 1992. Expression, purification, and properties of the plasma membrane Ca^{2+} pump and of its N-terminally truncated 105-kDa fragment. *J Biol Chem 267*:24476–34484.

Komiya H, Yeates TO, Rees DC, Allen JP, Feher G. 1988. Structure of the reaction center from *Rhodobacter sphaeroides* R-26 and 2.4.1: Symmetry relations and sequence comparisons between different species. *Proc Natl Acad Sci USA 85*:9012–9016.

Kosk-Kosicka D. 1990. Comparison of the red blood cell Ca^{2+}-ATPase in ghost membranes and after purification. *Mol Cell Biochem 99*:75–81.

Krebs J, Buerkler J, Guerini D, Brunner J, Carafoli E. 1984. 3-(Trifluoromethyl)-3-(*m*-[^{125}I]iodophenyl)diazirine, a hydrophobic, photoreactive probe, labels calmodulin and calmodulin fragments in a Ca^{2+}-dependent way. *Biochemistry 23*:400–403.

Kyte J, Doolittle RF. 1982. A simple method for displaying the hydropathic character of a protein. *J Mol Biol 157*:105–132.

Laurière M. 1993. A semidry electroblotting system efficiently transfers both high and low molecular weight proteins separated by SDS-PAGE. *Anal Biochem 212*:206–211.

Lüthy R, Eisenberg D. 1992. Protein. In: Gribskov M, Devereux J eds. *Sequence analysis primer.* New York: Freeman. pp 61–87.

Lutsenko S, Kaplan JH. 1995. Organization of P-type ATPases: Significance of structural diversity. *Biochemistry 34*:15607–15613.

Meister H, Bachofen R, Semenza G, Brunner J. 1985. Membrane topology of light-harvesting protein B870-alpha of Rhodospirillum rubrum G-9+. Amino acid residues in contact with the lipid bilayer as inferred from labeling with photogenerated carbenes. *J Biol Chem 260*:16326–31.

Møller JV, Juul B, le Maire M. 1996. Structural organization, ion transport, and energy transduction of P-type ATPases. *Biochim Biophys Acta 1286*:1–51.

Neuhoff V, Arold N, Taube D, Ehrhardt W. 1988. Improved staining of proteins in polyacrylamide gels including isoelectric focusing gels with clear background at nanogram sensitivity using Coomassie brilliant blue G-250 and R-250. *Electrophoresis 9*:255–262.

Penniston JT, Enyedi A. 1994. Plasma membrane Ca^{2+} pump: Recent developments. *Cell Physiol Biochem 4*:148–159.

Persson B, Argos P. 1994. Prediction of transmembrane segments in proteins utilising multiple sequence alignments. *J Mol Biol 237*:182–192.

Peterson GL. 1977. A simplification of the protein assay method of Lowry et al. which is more generally applicable. *Anal Biochem 83*:346–356.

Popot JL, Engelman DM. 1990. Membrane protein folding and oligomerization: The two-stage model. *Biochemistry 29*:4031–4037.

Rao US, Hennessey JP, Scarborough GA. 1991. Identification of the membrane-embedded regions of the *Neurospora crassa* plasma membrane H^+-ATPase. *J Biol Chem 266*:14740–14746.

Rees DC, DeAntonio L, Eisenberg D. 1989. Hydrophobic organization of membrane proteins. *Science 245*:510–513.

Rost B, Casadio R, Fariselli P, Sander C. 1995. Transmembrane helices predicted at 95% accuracy. *Protein Sci 4*:521–533.

Rost B, Fariselli P, Casadio R. 1996. Topology prediction for helical transmembrane proteins at 86% accuracy. *Protein Sci 5*:1704–1718.

Rost B, Sander C. 1993. Prediction of protein secondary structure at better than 70% accuracy. *J Mol Biol 232*:584–599.

Rost B, Sander C. 1994. Combining evolutionary information and neural networks to predict protein secondary structure. *Proteins Struct Funct Genet 19*:55–72.

Roufogalis BD, Villalobo A. 1989. The (Ca^{2+} + Mg^{2+})-ATPase. Purification and reconstitution. In: Raess BU, Tunnicliff G eds. *The red cell membrane, a model for solute transport.* New Jersey: Humana Press. pp 76–83.

Sander C, Schneider R. 1991. Database of homology-derived protein structures and the structural meaning of sequence alignment. *Proteins Struct Funct Genet 9*:56–68.

Schägger H, von Jagow G. 1987. Tricine-sodium dodecyl sulfate-polyacrylamide gel electrophoresis for the separation of proteins in the range from 1 to 100 kDa. *Anal Biochem 166*:368–379.

Sipos L, von Heijne G. 1993. Predicting the topology of eukaryotic membrane proteins. *Eur J Biochem 213*:1333–1340.

Stegmann T, Delfino JM, Richards FM, Helenius A. 1991. The HA2 subunit of influenza hemagglutinin inserts into the target membrane prior to fusion. *J Biol Chem 266*:18404–18410.

Stokes DL, Taylor WR, Green NM. 1994. Structure, transmembrane topology and helix packing of P-type ion pumps. *FEBS Lett 346*:32–38.

Strehler EE, James P, Fischer R, Heim R, Vorherr T, Filoteo AG, Penniston JT, Carafoli E. 1990. Peptide sequence analysis and molecular cloning reveal two calcium pump isoforms in the human erythrocyte membrane. *J Biol Chem 265*:2835–2842.

Tishler PV, Epstein CJ. 1968. A convenient method of preparing polyacrylamide gels for liquid scintillation spectrometry. *Anal Biochem 22*:89–98.

Toyoshima C, Sasabe H, Stokes DL. 1993. Three-dimensional cryo-electron microscopy of the calcium ion pump in the sarcoplasmic reticulum membrane. *Nature 362*:467–471.

von Heijne G. 1994. Membrane proteins: From sequence to structure. *Annu Rev Biophys Biomol Struct 23*:167–192.

Wallace BA, Cascio M, Mielke DL. 1986. Evaluation of methods for the prediction of membrane protein secondary structures. *Proc Natl Acad Sci USA 83*:9423–9427.

White BM, Howard S, Cohen SG, Cohen JB. 1991. The hydrophobic photoreagent 3-(trifluoromethyl)-3-*m*-([^{125}I] iodophenyl) diazirine is a novel noncompetitive antagonist of the nicotinic acetylcholine receptor. *J Biol Chem 266*:21595–21607.

Zurini M, Krebs J, Penniston JT, Carafoli E. 1984. Controlled proteolysis of the purified Ca^{2+}-ATPase of the erythrocyte membrane. A correlation between the structure and the function of the enzyme. *J Biol Chem 259*:618–627.

Zvaritch E, James P, Vorherr T, Falchetto R, Modyanov N, Carafoli E. 1990. Mapping of functional domains in the plasma membrane Ca^{2+} pump using trypsin proteolysis. *Biochemistry 29*:8070–8076.